



**HAL**  
open science

## New generation of composite substrates based on a layer of LiTaO<sub>3</sub> on silicon for surface acoustic waves components

Alexandre Clairet, Emilie Courjon, Thierry Laroche, Florent Bernard, Alexandre Raveski, Eric Michoulier, Gabrielle Aspar, Christophe Didier, Isabelle Huyet, Eric Butaud, et al.

### ► To cite this version:

Alexandre Clairet, Emilie Courjon, Thierry Laroche, Florent Bernard, Alexandre Raveski, et al.. New generation of composite substrates based on a layer of LiTaO<sub>3</sub> on silicon for surface acoustic waves components. Forum Acusticum, Dec 2020, Lyon, France. pp.2527-2533, 10.48465/fa.2020.0157 . hal-03231876

**HAL Id: hal-03231876**

**<https://hal.science/hal-03231876>**

Submitted on 21 May 2021

**HAL** is a multi-disciplinary open access archive for the deposit and dissemination of scientific research documents, whether they are published or not. The documents may come from teaching and research institutions in France or abroad, or from public or private research centers.

L'archive ouverte pluridisciplinaire **HAL**, est destinée au dépôt et à la diffusion de documents scientifiques de niveau recherche, publiés ou non, émanant des établissements d'enseignement et de recherche français ou étrangers, des laboratoires publics ou privés.

# New generation of composite substrates based on a layer of $\text{LiTaO}_3$ on silicon for surface acoustic waves components

Alexandre Clairet<sup>1</sup>, Émilie Courjon<sup>1</sup>, Thierry Laroche<sup>1</sup>, Florent Bernard<sup>1</sup>, Alexandre Raveski<sup>1</sup>,  
Éric Michoulier<sup>1</sup>, Gabrielle Aspar<sup>1</sup>, Christophe Didier<sup>2</sup>, Isabelle Huyet<sup>2</sup>, Éric Butaud<sup>2</sup>, Aymen  
Ghorbel<sup>2</sup>, Brice Tavel<sup>2</sup>, Alexis Drouin<sup>2</sup>, Julien Garcia<sup>1</sup>, Sylvain Ballandras<sup>1</sup>

<sup>1</sup> freqn|sys, 18 rue Alain Savary, 25000 Besançon, France

<sup>2</sup> SOITEC, Parc des Fontaines, 38190 Bernin, France

alexandre.clairet@freqnsys.fr

## ABSTRACT

This paper describes a new generation of composite substrates dedicated to advanced surface acoustic wave (SAW) devices. For very long years, SAW applications (filters, resonators, sensors) have been developed on single crystal materials. The Piezoelectric-On-Insulator (POI) structure which combines highly coupled single crystals with silicon offers today unique properties to meet the challenges of modern telecommunications. This paper proposes a review of the concept and figures of merit on test vehicles.

## 1. INTRODUCTION

The development of new generations of telecommunication systems requires more and more components and radio-frequency (RF) modules to select and process signals supporting the information. The most used solution for this kind of application is always based on the principle of surface acoustic waves (SAW) and its associated components, taking into account their unique spectral quality (insertion losses, out of band rejection, group delay...), their design flexibility and their compactness for L- and S-bands. Although still commonly used today, filters on single-crystals such as Lithium Tantalate ( $\text{LiTaO}_3$ ) and Lithium Niobate ( $\text{LiNbO}_3$ ) cannot be used for future RF modules since the thermal stability of these substrates is far from being adapted to meet the challenges of modern telecommunications [1].

As a consequence, disruptive solutions are needed and strong efforts are deployed to develop them [2]. Although investigated for years without real commercial breakthrough [3], the combination of piezoelectric films and Silicon is now receiving a very strong interest.

Murata has already demonstrated the capabilities of filters based on combination of  $\text{LiTaO}_3$  layers and Silicon [4], although the technology sounds rather difficult to control industrially. The use of advanced composite substrates actually offers more than simply an alternative to single crystals with improved temperature stability [5], but a real paradigm change. Leaky SAWs (SAW with a part of radiation in the bulk) usually

exploited for RF filters [6] can still be used, but the use of guided waves without any radiation leakage opens the way to new design approaches. In particular, these wafers receive a very interest since the wave properties are influenced by material stack nature and dimensions.

In this paper, we propose to present the concept of this kind of structure, named POI for Piezoelectric-On-Insulator from wave-guides principle to the technology allowing for manufacturing these composite substrates, the so-called Smart Cut™ technology. Then, theoretical characteristics of POI are given and experimental SAW figures of merit measured on test vehicles are reported. Finally, examples of applications are also depicted in order to highlight the potential of this new technological solution for telecommunications or wireless sensors.

## 2. CONCEPT AND INTERESTS OF WAVE-GUIDES FOR SAW

Crystal surface represents a natural wave guide for elliptically polarized waves. The description of the corresponding concepts has been detailed in many textbooks [7, 8], as well as the theory and implementation of SAW devices. By elsewhere, the invention of interdigitated transducers (IDT) has enabled the technological development of such devices with miniaturized dimensions, compatible with signal processing tools and capable to be integrated in complex front-end modules.

The main interests in the development of wave-guides structures are:

- suppression of radiation losses,
- using shear waves expected to reduce losses,
- improvement of the electromechanical coupling,
- reduction of thermal expansion and TCF (temperature coefficient of frequency),
- possible mode acceleration (to increase frequency),
- substrate linearity, resistivity, thermal conductivity and compatibility with CMOS electronics.

By computing the complex effective permittivity, we can characterize the electrical response of a medium to a charge distribution at an interface and detect the excited modes. The poles also provide information on the physical nature of the wave. If the

pole is purely real, the mode is guided at the interface without radiation of energy within the material: it is a “true” mode. If the pole is complex, a part of the energy is lost by radiation: it is a pseudo-mode. Figure 1 compares the spectral response of such a wave-guide combining (YXl)/42° LiTaO<sub>3</sub> with Silicon and bulk LiTaO<sub>3</sub>. Although a second contribution is seen here near 5400 m/s, the spectral response of the composite wafer is mainly composed of a unique mode (blue and orange curves). This main mode is then purely real. As shown in this figure, the amplitude of the main pole corresponding to the guided wave is much larger than the LSAW (Leaky SAW) signature for the bulk (purple and green curves). Its velocity is a bit smaller (4056 m/s against 4115 m/s) due to the presence of SiO<sub>2</sub> at the LiTaO<sub>3</sub>/Si interface. The use of optimized silicon orientations is useful to limit the impact of the discussed secondary mode [16].

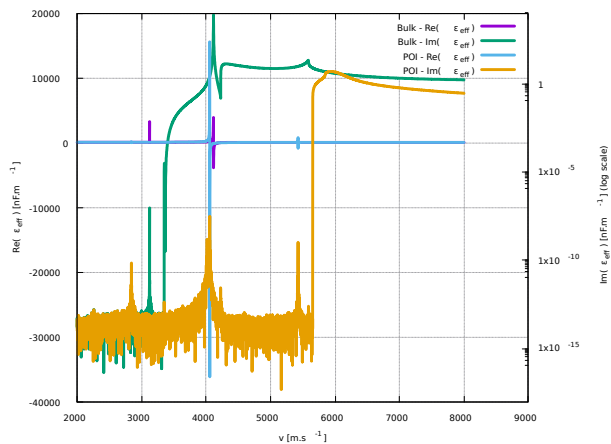


Figure 1: Effective permittivities at the surface of a bulk (YXl)/42° LiTaO<sub>3</sub> and a 600 nm thick (YXl)/42° LiTaO<sub>3</sub> layer on 500 nm thick SiO<sub>2</sub> on (100) Si semi-infinite composite substrate at 1.6 GHz (POI). The imaginary part is plotted in log scale.

As explained previously, another interest of such kind of composite substrate is to reduce the TCF of surface waves devices. The TCF is composed at first order of a contribution relative to elastic properties and another contribution due to thermal expansion. In the case of single crystal substrates with low thermal expansion, their TCF is quite large and does not achieve this objective. In the case of POI wafers, the thermal coefficient of expansion (TCE) part of the TCF is artificially suppressed by combining a single piezoelectric top layer with a high crystal quality substrate with very low TCE. To obtain an effect due to the substrate-induced TCE reduction, the top piezoelectric layer must be thin enough (about or less than 10 wavelengths) and the substrate must be 100 wavelength thick or more. The material used as substrate can be for example Silicon Oxide (TCE < 1,5 ppm/K), Silicon Carbide (~ 4 ppm/K), Sapphire (TCE ~ 4 ppm/K) or Silicon (TCE ~ 2.5 ppm/K) [17] while the TCE of LiTaO<sub>3</sub> is 4 (//) -16 (⊥) ppm/K.

### 3. PIEZO-ON-INSULATOR (POI) WAFERS

As said previously, the idea consisting in the combination of substrate with piezoelectric top layer to develop wave-guides has been investigated by several groups at the end of the passed century [3, 9, 10], when technology finally allowed for such developments at industrial level.

The manufacturing of POI has been depicted in several publications [11]. Although very generic and applicable to almost any crystal combination, the selected piezoelectric layer material is Lithium Tantalate as the best trade-off between electromechanical coupling strength, resonance quality and thermal stability. As already shown in literature [12], combining single rotation LiTaO<sub>3</sub> cuts (IEEE std-176 notation (YXl)/θ with θ corresponding to standard single crystal cut angle around X axis) and Silicon bonded with SiO<sub>2</sub> allows for significant reduction of frequency-temperature drift of the shear mode guided on such substrate.

Wafer bonding technologies have experienced significant improvements in recent years and can be efficiently implement to provide composite wafers meeting industrial requirements. The most efficient approach is based on the so-called Smart Cut™ technology [13]. Smart-Stacking™ technology can be implement as well, but it will not be explained here. The manufacturing principle of such wafers is shown in Figure 2.

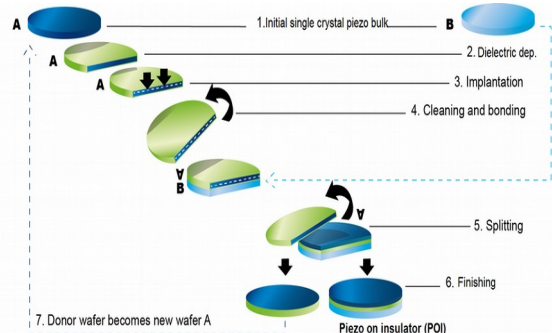


Figure 2: Smart Cut™ principle and processing flow chart for POI wafers.

The principle of the technology is based on ion implantation with particle energy and flow enabling one to control the depth of max implantation density. After implantation, the surface to be bonded is cleaned and prepared to exhibit hydrophilic properties according to the molecular bonding process. Once LiTaO<sub>3</sub> and Si wafers bounded together, thermal processes are applied, yielding a progression of physical defects at this depth due to ion mobility and affinity in such way that finally the implanted layer is separated from the initial support at the end of the process. A high quality surface is recovered afterwards by chemical-mechanical polishing (CMP) and the LiTaO<sub>3</sub> layer is cured to obtain initial Lithium Tantalate properties.

The configuration uses here to demonstrated the interest of such stack consist of a layer of  $\text{LiTaO}_3$  bonded onto a (100) Si substrate via a  $\text{SiO}_2$  layer (see Figure 4), but we can imagine others substrates like Sapphire or Lithium Tantalate. The  $\text{SiO}_2$  layer is useful to improve the temperature compensation and is a key point to increase the electromechanical coupling factor. An example of 150 mm diameter (YXl)/42°  $\text{LiTaO}_3$ // $\text{SiO}_2$ //Si POI wafer is reported in Figure 3, showing the very high uniformity ( $\pm 3\%$  of the nominal thickness) and integrity of the final product.

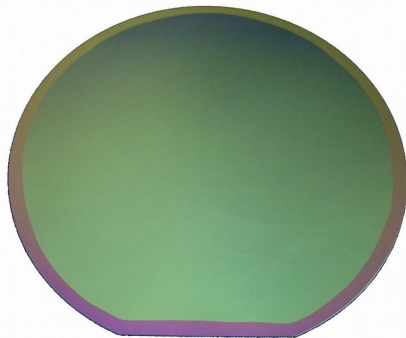


Figure 3: Very high quality full wafer  $\text{LiTaO}_3$  film transfer, 150 mm diameter wafer with SAW grade surface finishing.

#### 4. THEORETICAL CHARACTERISTICS

Computations based on Green's functions of stratified media (see Figure 4) have been conducted for identifying trends of guided wave characteristics on our composite substrates.

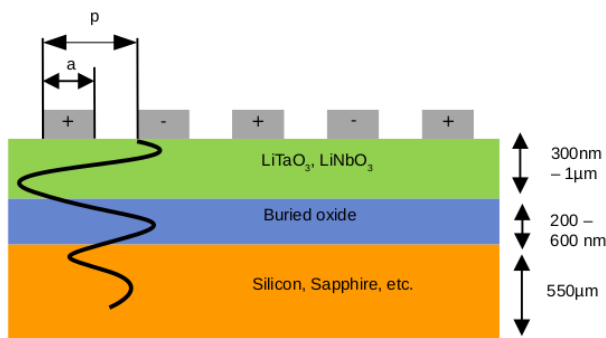


Figure 4: Standard material stack for SAW devices based on single crystal bonded on non-piezoelectric single crystal substrate

It is noted in Figure 5 that, in this configuration, due to the difference of acoustic properties between Si and  $\text{LiTaO}_3$ , the dispersion effect is particularly visible for small frequency· $\text{LiTaO}_3$  thickness products ( $f \cdot t$  smaller than 1000 m/s). As said previously, we observe the effect of the  $\text{SiO}_2$  thickness on the velocity and the  $k_s^2$ . Higher the thickness, higher the coupling, but lower the velocity. The thickness of  $\text{SiO}_2$  has to be defined in order

to have a compromise between coupling and velocity. As we can note, for some configurations, the electromechanical coupling coefficient can be higher than 12% compared to 6% for LSAW on bulk  $\text{LiTaO}_3$ . Concerning the phase velocity, POI wafers allow to reach higher velocity than bulk  $\text{LiTaO}_3$  (until 5600 m/s instead of 4140 m/s) for some specific configurations.

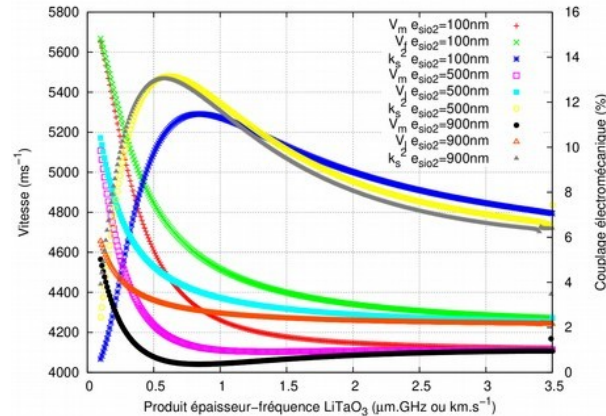


Figure 5: Phase velocity and electromechanical coupling coefficient of the fundamental pure shear wave propagating on top of (YXl)/42°  $\text{LiTaO}_3$ // $\text{SiO}_2$ //Si composite wafer for various  $\text{SiO}_2$  and  $\text{LiTaO}_3$  thicknesses.

Therefore, the  $\text{LiTaO}_3$  thickness has to be precisely controlled to optimize the mode stability. A particular attention must be also dedicated to the optimization of  $\text{SiO}_2$  thickness to control the TCF which dependent on this parameter as shown in Figure 6.

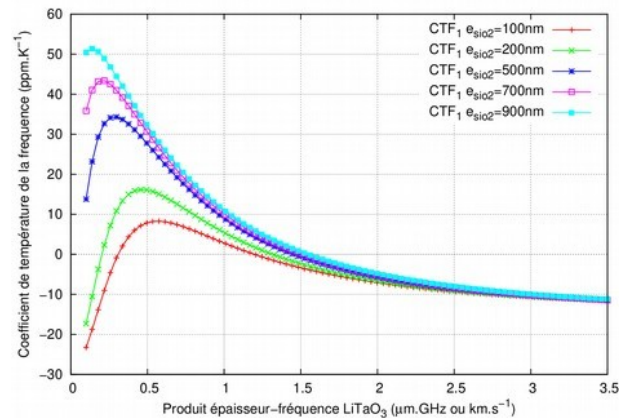


Figure 6: First order TCF of the fundamental pure shear wave propagating on top of (YXl)/42°  $\text{LiTaO}_3$ // $\text{SiO}_2$ //Si composite wafer for various  $\text{SiO}_2$  and  $\text{LiTaO}_3$  thicknesses.

Thanks to this curve, we note that optimization of thicknesses is a key point. Therefore, the 0 ppm/K sensitivity can be achieved for a given frequency using optimized thicknesses.

## 5. EXPERIMENTAL FIGURES OF MERIT

The characterization of SAW mode on these POI composite substrates has been achieved using single port resonators at different frequencies. Figure 7 shows the archetype of resonators used for our study. The structure is composed of a 120 finger-pair IDT between 20-electrode mirrors on each side. The acoustical aperture is  $40\lambda$ -long. The test devices have a period  $p = 1.2 \mu\text{m}$  and  $p = 1.4 \mu\text{m}$ . The deposited electrodes are in Aluminum with a thickness of 150 nm and  $a/p$  ratio equals to 0.5.

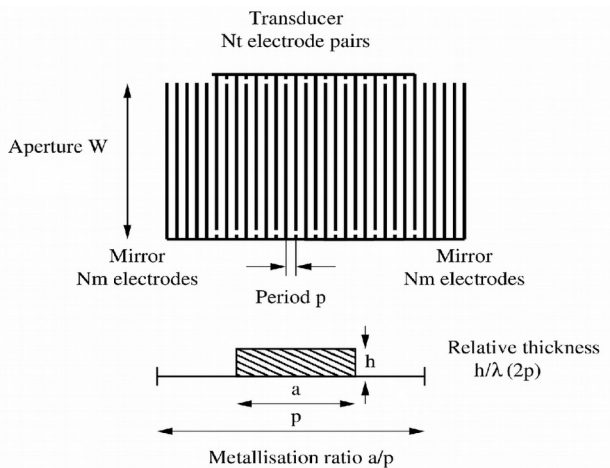


Figure 7: Typical single-port resonator used for characterizing SAW properties.

The extraction of figures of merit is done from the measured S-parameters ( $S_{11}$  in our case) converted in complex admittance ( $Y_{11}$ ) and complex impedance ( $Z_{11}$ ). Some of the extracted figures of merit are: the resonance ( $f_r$ ) and anti-resonance ( $f_a$ ) frequencies, the electromechanical coupling factor ( $k_s^2$ ), the quality factors at resonance ( $Q_r$ ) and anti-resonance ( $Q_a$ ), the impedance ratio... The conductance (real part of the admittance,  $G$ ) and the resistance (real part of the impedance,  $R$ ) of the device excited at 1.6 GHz ( $p = 1.2 \mu\text{m}$ ) are reported in Figure 8.

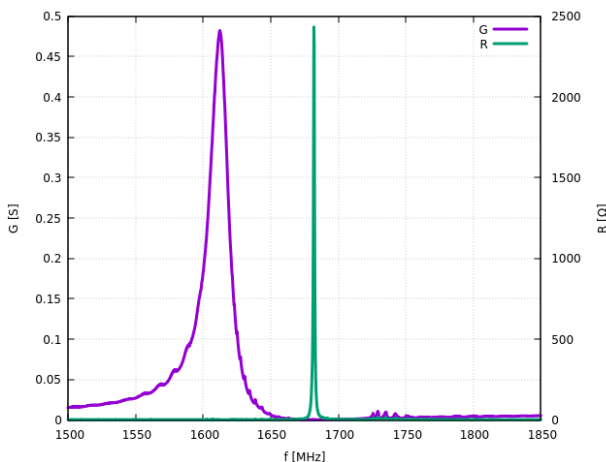


Figure 8: Characterization results for the device excited near 1,6 GHz ( $p = 1.2 \mu\text{m}$ ) on 600 nm  $\text{LiTaO}_3$ /500 nm  $\text{SiO}_2$ /(100) Si

Due to a non-optimized design, we note the presence of some transverse modes before and after the resonance. Nevertheless, these curves allow us to determine a coupling  $k_s^2$  equals to 8.1% and quality factors  $Q_r = 100$  and  $Q_a = 2570$ . For LSAW on bulk  $\text{LiTaO}_3$  for exactly the same device and at the same frequency, we measure  $k_s^2 = 6\%$ ,  $Q_r \sim 150$  and  $Q_a \sim 935$  (see Figure 9).

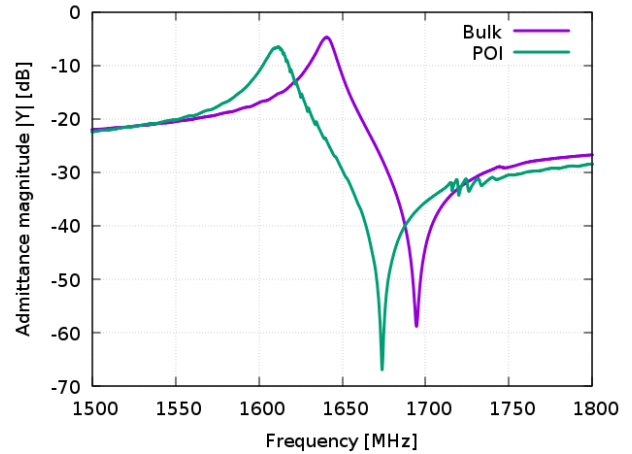


Figure 9: Admittance magnitude versus frequency for a single-port resonator at 1,6 GHz on POI and bulk  $\text{LiTaO}_3$ .

At 1.4 GHz ( $p = 1.4 \mu\text{m}$ ), the results are:  $k_s^2 = 8.5\%$ ,  $Q_r = 100$  and  $Q_a = 3060$ . If we now study the thermal sensitivity of these two kind of substrates (POI and bulk), we obtain the Figure 10. These curves are determined at 2.4 GHz pour POI and 1.6 GHz for  $\text{LiTaO}_3$  bulk.

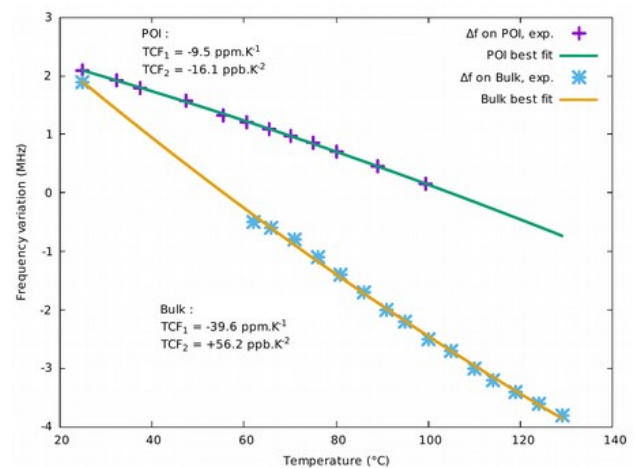


Figure 10: TCF of the interested mode between POI and bulk  $\text{LiTaO}_3$ .

Thanks to this combination of materials, absolute TCF values equal to 9.5 ppm/K have been obtained in this example compared to the usual 39.6 ppm/K values of  $\text{LiTaO}_3$  single crystal substrates. These results well illustrate the advantage of POI structures in terms of figures of merit and temperature compensation.

## 6. APPLICATIONS TO FILTERS AND SENSORS

### 6.1 SAW filters

Based on this characterization work, we have designed a first SAW filter. This filter corresponds to a GPS application and more precisely to L1 encoding band filtering. The operating frequency of this device is 1575.42 MHz. Our SAW filter uses a SAW-ladder architecture and the wafer is based on a 30  $\mu\text{m}$  LiTaO<sub>3</sub> (YXI)/42° layer onto a 500 nm SiO<sub>2</sub> layer onto a 650  $\mu\text{m}$  Si substrate.

The first step consists in determining SAW properties of series and parallel resonators before finalizing the filter design. Their electrical responses were measured and some figures of merit extracted. Table 1 summarizes the averaged values of the wave velocity, the resonance and anti-resonance frequencies, the coupling factor and the quality factor for each resonator (considering 10 resonators measurements).

**Table 1.** Figures of merit of the series and parallel resonators

Resonator	Series	Parallel
$v$ [m/s]	3934.8	3905.1
$f_r$ [MHz]	1567.67	1517.13
$f_a$ [MHz]	1605.37	1554.59
$k_s^2$ [%]	4.87	5.00

The final design of the filter was made to meet the typical characteristics for this kind of application. Then, the experimental  $S_{12}$  parameter and phase of our filter were measured and are reported in Figure 11.

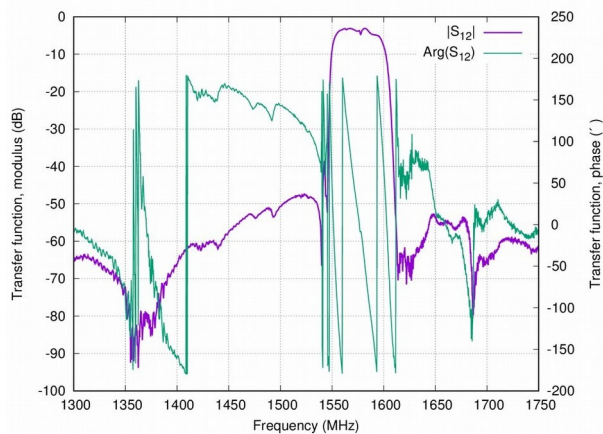


*Figure 11: Wide band transfer function  $|S_{21}|$  of our filter.*

The bandpass is found near 45 MHz (corresponding to a 3% relative bandpass) with insertion losses near 3.5 dB and a typical far field rejection of 45 dB. The device is capable to enter a 3.0  $\times$  3.0 mm<sup>2</sup> ceramic Surface Mount Package (SMP), although the foot-print of the initial version was larger. Finally, the electrical response of the filter was measured at various temperatures between 25°C and 85°C. Figures 12 and 13 show the experimental  $S_{12}$  and  $S_{11}$  parameters for each temperature.

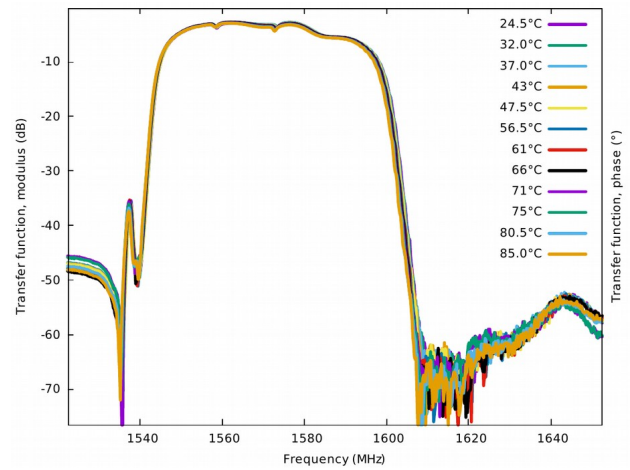


*Figure 12: Transfer function  $|S_{12}|$  versus temperature.*

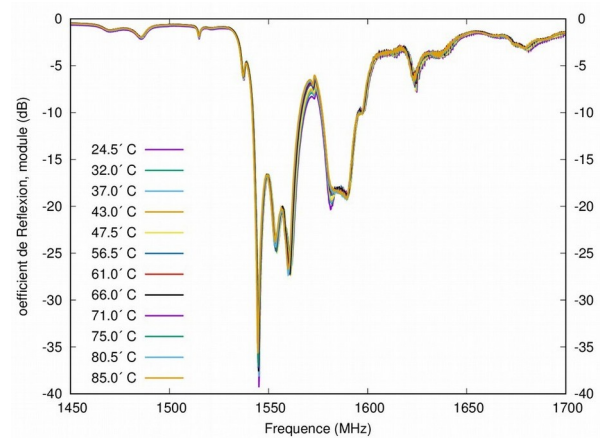


*Figure 13: Reflection coefficient  $|S_{11}|$  versus temperature.*

Thanks to these results, we can conclude that the typical temperature stability is better than -9 ppm/K.

### 6.2 SAW sensors

Although mainly developed for filter applications, POI is also interesting for SAW wireless sensors thanks to its electromechanical coupling factor and a better control of temperature sensitivity (TCF<sub>1</sub> ranging from 20 to less than 5 ppm/K, lower than LiNbO<sub>3</sub> or LiTaO<sub>3</sub> bulk wafers) which allows possibility to interrogate more sensors in the same band. Another interesting point, the reflection coefficient per electrode is higher for POI than for other substrates which improves the compactness of SAW sensors. In order to characterize the interest of composite substrates for sensor applications, we use another kind of single-port resonator. The design is close to the one shown in Figure 7, but a gap between the transducer and the mirrors is added to create a free space cavity (see Figure 14).

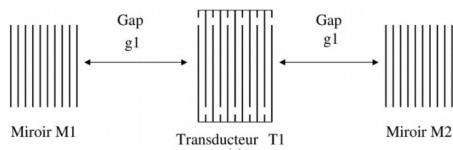


Figure 14: General principle of SAW device for sensor application.

In this example, the length of the gap is 350  $\mu\text{m}$ . In that way, each reflection of the wave will appear in the electrical response of the transducer as a peak. Then, the gap between each peak corresponds to the distance of wave traveling (two times the gap). If this distance changes (due to external environmental), the frequency distance between each of these peaks will be closer or further according to the environment, like temperature or stress for example. This modification then is studied to determine the physical parameter to measure.

In the case of SAW sensors, the use of POI substrates is interesting in order to have a better definition of reflection peaks thanks to a better quality factor. The higher the Q, the narrower the peaks and the better the signature and the detection of each peak. Usually, for a same material, we have a  $k_s^2 \cdot Q$  product constant. One the interest of POI is the possibility to have a simultaneous increase of the quality factor and the coupling coefficient compared to a bulk substrate.

The response of this kind of device near 1.6 GHz on a 680 nm LiTaO<sub>3</sub> (YXl)/50°// 500 nm SiO<sub>2</sub> // 1  $\mu\text{m}$  pSi/Si substrate is shown in Figure 15.

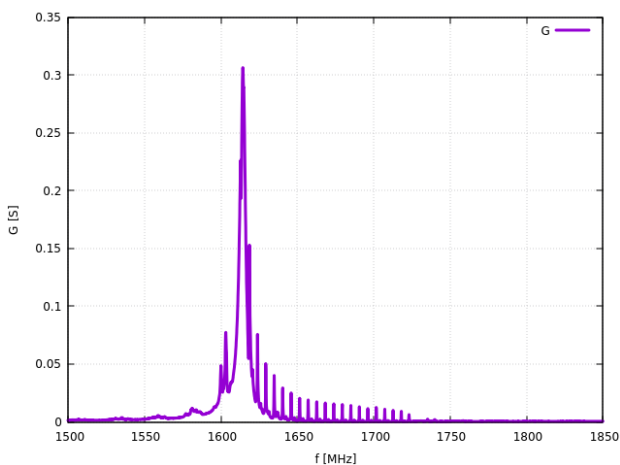


Figure 15: Experimental conductance of a single-port resonator with a gap between transducer and mirrors.

The reflection peaks are easily visible in this curve. Using freq|n|sys interrogation system (see Figure 16), we are able to monitor and determine the temperature or the stress for example using the sensor response changes. For temperature sensor, the operating temperature range is between -60°C and 200°C by using

vacuum sealing. In a “classical” SAW sensor, the measurement is done with two resonators in order to have a differential measurement. By using POI wafers, the use of only one resonator to perform this differential measurement is then achievable [18].

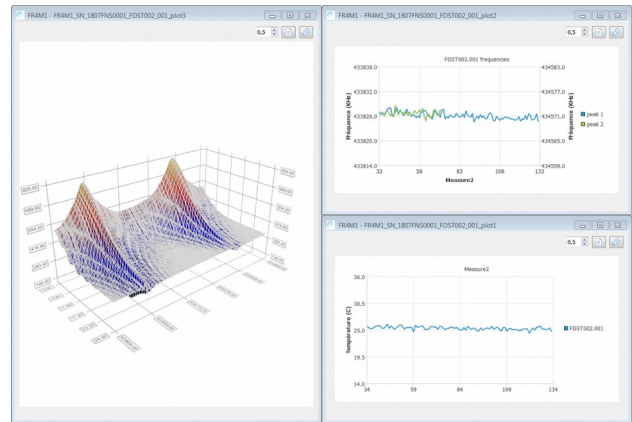


Figure 16: Example of interrogation of a temperature sensor. Monitoring of 2 reflection peaks.

## 7. CONCLUSION

In this paper, a presentation of composite Piezoelectric-On-Insulator substrates and their applications has been proposed. The principle of this kind of wafer is based on the realization of wave-guides for SAW thanks to a stack of materials with specific properties. Through characterizations and applications, the interests of this kind of wafer have been defined. We can cite:

- Increase of the coupling factor (12% theoretically, higher than 9% experimentally)
- Increase of the quality factor (more than 3000)
- Increase of the phase velocity (up to 5600 m/s)
- Reduction of temperature sensitivity (lower than 10 ppm/K and 0 ppm/K achievable)
- Better compactness of devices compared to bulk materials

Single-port resonators at 1.4 GHz and 1.6 GHz have shown a coupling factor higher than 8% (better than for bulk LiTaO<sub>3</sub>) and quality factors increased compared to single crystal wafers which allow us to achieve innovative filters as well as sensors and respond to new challenges. The thermal sensitivity also is improved by optimizing the thicknesses of Lithium Tantalate and SiO<sub>2</sub> layers. In this document, examples of SAW filters and sensors have been reported showing the interest of POI for each configuration.

## 8. REFERENCES

- [1] K. C. Wagner, C. Bauer, T. Bauer, I. Bleyl and C. Eggs: “Technological Innovations in SAW Components for Frontend Modules with High

- Function Density,” *Proc. of the 7th International Symposium on Acoustic Wave Devices for Future Mobile Communication Systems*, Chiba, pp. 18–22, 2018.
- [2] Y. Hori, H. Kobayashi, K. Tohyama, Y. Iwasaki and K. Suzuki: “A Hybrid Substrate for a Temperature-Compensate Surface Acoustic Wave Filter,” *IEEE Ultrason. Symp.*, pp. 2631–2634, 2009.
- [3] K. Eda, K. Onishi and S. Seki: “Surface Acoustic Wave device having a lamination structure,” *United States Patent US005446330A*, 1995.
- [4] H. Iwamoto, T. Takai, Y. Takamine, T. Nakao, T. Fuyutsume, M. Hiramoto and M. Koshino: “IHP SAW Technology and its Application to Filter Devices in Mobile Terminals,” *Proc. of the 7th International Symposium on Acoustic Wave Devices for Future Mobile Communication Systems*, Chiba, pp. 133–144, 2018.
- [5] J. Hayashi, M. Gomi, M. Suzuki, S. Kakio, H. Suzuki, T. Yonai, K. Kishida and J. Mizuno: “High-Coupling Leaky SAWs on LiTaO<sub>3</sub> Thin Plate Bonded to Quartz Substrate,” *IEEE Ultrason. Symp.*, 2017.
- [6] O. Kawachi, S. Mineyoshi, G. Endoh, M. Uedo, O. Ikata, K. Y. Hashimoto and M. Yamaguchi: “Optimal cut for leaky SAW on LiTaO<sub>3</sub> for high performance resonators and filters,” *IEEE Trans. Ultrason. Ferroelectr. Freq. Control*, pp. 1442–1448, 2001.
- [7] S. Inoue and M. Solal: “Guided SAW device,” *US patent application US2018159495 (A1)*, 2018.
- [8] D. Royer, and E. Dieulesaint: *Elastic waves in solids*, Springer Verlag, 2000.
- [9] A. Namba, M. Sugimoto, T. Ogura, Y. Tomita and K. Eda: “Direct bonding of piezoelectric crystal onto silicon,” *Applied Phys. Letters*, vol. 67, p. 3275, 1995.
- [10] M. Solal, T. Pastureauud, S. Ballandras, B. Aspar, B. Biasse, W. Daniau, J.-M. Hodé, S. Calisti and V. Laude: “Oriented lithium niobate layers transferred on 4” [100] silicon wafer for RF SAW devices,” *2002 IEEE Ultrason. Symp.*, pp. 131–134, 2002.
- [11] M. Gorisse *et al.*: “Oriented single-crystal LiTaO<sub>3</sub> thin film on silicon for high performances SAW components,” *2018 IEEE International Ultrason. Symp.*, pp. 1–4, 2018.
- [12] S. Ballandras *et al.*: “New generation of SAW devices on advanced engineered substrates combining piezoelectric single crystals and silicon,” *2019 Joint conference of the IEEE International Freq. Contr. Symp. and European Freq. and Time Forum*, pp. 1–6, 2019.
- [13] B. Aspar and A. J. Auberton-Hervé: “Smart Cut™: the technology used for high volume SOI wafer production,” *Silicon wafer bonding technology for VLSI and MEMS applications*, S. S. Iyer and A. J. Auberton-Hervé, Ed. INSPEC EMIS Processing Series 1, p. 35, 2002.
- [14] C. Lagahe-Blanchard and B. Aspar: “Wafer stacking: key technology for 3D integration,” *2009 IEEE International SOI Conference*, pp. 1–4, 2009.
- [15] J. J. Campbell and W. R. Jones: “A method for estimating optimal crystal cuts and propagation directions for excitation of piezoelectric surface waves,” *IEEE Trans. on Sonics and Ultrason.*, vol. 15, no. 4, pp. 20-99217, 1968.
- [16] D. Morgan: *Surface acoustic wave filters*, 2<sup>nd</sup> edition, Academic Press, 2007.
- [17] *American Institute of Physics handbook*, 3<sup>rd</sup> edition, E. D. Gray, McGraw-Hill, 1972.
- [18] S. Ballandras, W. Daniau and T. Laroche: “Surface Acoustic Wave sensor that can be polled remotely”, Patent EP3032742.